Spectroscopic and Transport Behavior of HAB-6FDA Thermally Rearranged (TR) Nanocomposite Membranes

Harsh Patel
The Maharaja Sayajirao University of Baroda
NAVEEN KUMAR ACHARYA (✉ sarnavee@gmail.com)
Maharaja Sayajirao University of Baroda https://orcid.org/0000-0002-9206-8891

Research Article

Keywords: Membranes, Nanocomposite, Gas Permeability, Selectivity, X-ray diffraction

Posted Date: November 8th, 2021

DOI: https://doi.org/10.21203/rs.3.rs-1030872/v1

SPECTROSCOPIC AND TRANSPORT BEHAVIOR OF HAB-6FDA THERMALLY REARRANGED (TR) NANOCOMPOSITE MEMBRANES

H. D. Patel, N. K. Acharya*

Corresponding Author: sarnavee@gmail.com

Applied Physics Department, Faculty of Technology and Engineering, The M.S. University of Baroda, Vadodara 390 001, INDIA

Nanocomposite membranes are a class of innovative filtering materials made up of nanofillers embedded in a polymeric or inorganic oxide matrix that functionalized for the membrane. Thermally rearranged (TR) polymers are found to have a good blending of selectivity and permeability. Chemical iridization is a process for used to make HAB-6FDA polyimide from 3,3 dihydroxy-4,4 diamino-biphenyl (HAB) & 2,2-bis-(3,4-dicarboxyphenyl) hexafluoro propane dianhydride (6FDA). The sample is first changed from a pure polymer membrane to a silica nanofiller doped polymer layer and explain thermally rearrangement for gas permeability in polymer nanocomposite layers and its relationship with kinetic diameter of different gases. The selectivity is decreases as the permeability increases that shows on a trade-off relationship between permeability & selectivity. The CO_2 permeability of the HAB-6FDA TR polymers is greater than that of other classes of polymers by equal free volume and indicating that these TR polymers have free volume distribution that supports high permeability. Thermally rearranged polymer nanocomposite exhibits higher gas permeability than that of silica doped and pure polymer. The selectivity for H_2/N_2 and H_2/CO_2 gas pairs exceeds towards Robeson's upper bound limit and in case of H_2/CH_4 gas pair this limit were crossed the Robeson's upper bond limit. UV spectroscopy shows the change in transmission at higher wavelengths, while XRD show the reduction in FWHM with thermal treatment temperature. Polymer nanocomposite can be utilized to obtain high purity hydrogen gas for refinery and petrochemical applications.

Keywords: Membranes; Nanocomposite; Gas Permeability; Selectivity; X-ray diffraction

1. Introduction

Polymer nanocomposite development is becoming increasingly popular among material science. These new materials can be used for water purification, gas separation, fuel cells, drug delivery, nano-electronics, and other multidisciplinary research applications. The membrane-built separation method on polymer nanocomposite are received a lot of attention in the literature. The unique assets of nanoparticles have resulted in a novel form of composite membrane material. Membrane-based separation is widely used in businesses and laboratories expected to its minimal initial price, low energy consumption, as well as easy of use [1-5]. The structure of the host polymer is altered when inorganic nanoparticles are introduced into a polymer matrix, which increases separation assets [6].

The physicochemical assets of nanocomposite layers are manipulated to variable degrees by the type of filler and the nature of the host material [7-9]. The separation assets of carbon nanotube integrated pattern membranes. Apart from the benefits, membrane materials are nevertheless limited by the tradeoff relation of permeability-selectivity [10]. However, PIOFG (polyimide with ortho-functional group) demonstrates increased absorbency with no affecting selectivity [11]. In that way, precursor polyimide improvement for the ortho-functionality group gives other bonds to TR materials of membrane film properties. Furthermore, pure polyimides modified from replaced –OH groups of various functionalities to weaker hydrogen bonding groups. Previously considered polyimide ortho-functionalities are using a various type of synthesis methods. Some of the primary components like structures, atomic loads, and insufficient imidization would be presented through various imidization ways, significantly compound imidization. These variations observed in properties of ortho-functionality group may change after TR modifications. Hence, the methodology detailed in that experiment contains derivatized poly(hydroxide) using various experts to present other ortho-functional groups supplanting to –OH groups. Precursor polyimides have been used as the precursor of thermal rearrangement to manage the cost of superior TR films with applications in gas separation. A polymer–inorganic nanocomposite is made up of inorganic nanoparticles dispersed at the nanoscale point in a polymer pattern in a heterogeneous or homogeneous dispersion. The capacity of these materials to exceed the limits of the standard permeability–selectivity trade-off relationship [12-13] has been established.

As of later, observed another group of gas separation membrane films, thermally rearranged (TR) polymers obtained from precursor polyimides of ortho-positioned hydroxyl groups. The dense membrane mix with TR polymers gives high selectivity with high permeability as provided in the past by Robeson's 1991 or 2008 upper limit for H_2/CH_4 separation [17]. XRD is a method used in materials science to verify the crystallographic structure of a material. XRD operates with exposing a material plus X-rays & subsequently determining the concentrations and scattering angles of the X-rays that leave the information.

1.1. Temperature-Dependent Gas Permeability

Temperature-dependent gas permeability can be used to assess the activation energy used for permeation, diffusion, plus heat of sorption in pure polymer and blends [14,15]. The Van't Hoff relation [14] gives the activation energy for permeation as shown in Equation (1).

$$P = P_o \exp(-E_p/RT) \quad (1)$$

E_p = Activation energy for permeation, P = Permeability coefficient, R = Gas constant, P_0 = Pre-exponential factor, T = Operating temperature, P_0 =Pre-exponential factor the gas constant [16]. Different processes can be used to explain gas molecule transport over dense polymer nanocomposite membranes: Maxwell’s model, along with lowered permeability due to the use of impermeable filler particles that are roughly spherical. [17], Due to a change in the penetrant's diffusion coefficient, there is an increase in free volume and permeability. [18]. Depending on the functionality, a rise in solubility is associated with an increase in permeability because of interaction among penetrant gas and integrated nanoparticles [19]. Due to the development of gaps between nanoparticles and polymer chains, the permeability of the system is increased. [20].

1.2. Membrane Technology (MT)

Membrane technology has evolved into a respectable separation technology on the millennia. MT's key advantage is that it operates without the use of chemicals, uses extraordinarily little energy, and has simple and well-organized process conductions. The various applications of MT's is generally membrane used for Air protection, Water purification, Pharmacy, Medicine, Food technology, Soil Protection, Agriculture.

MT is a generic name for a variety of gas separation techniques, because a membranes is used in each of these activities, they are all of the same type. Membranes are increasingly being used to make process water from groundwater, surface water, or wastewater. Membranes are now a viable alternative to traditional procedures. The existence of semipermeable membranes is used in the membrane separation process.

The membrane functions as a highly selective filter, allowing gas to pass through while capturing suspended particles and other contaminants. There are several methods for allowing gases to pass through a membrane. High-pressure applications, retaining a concentration gradient on each side of the membrane, and introducing an electric potential are examples of these approaches.

Membranes occupy a space separated by a selective barrier. Certain gases flow through the membrane without being caught, whereas others are caught. Membrane filtration can replace flocculation, sediment purification, adsorption, extraction, and distillation. The membrane filtering process is defined by two factors: selectivity and permeability. Selectivity is measured using a metric known as retention or separation factor. Flux is a measure of permeability [21]. Figure 1 depicts the Membrane Filtration Process.

Membrane technology, with its high permeability and selectivity helps to achieve good performance in purification and separation technology. This technology is useful for environmental purification, energy storage, and other applications such as biopharmaceutical separation, pharmaceutical and medical product sterilizing, flue cell, reverse osmosis wastewater treatment, and the removal of big protein molecules from milk. Membrane-based purification and separation processes are less expensive and use less energy. Membrane materials such as polymers are frequently employed in mass transportation processes due to their high permeability and environmental friendliness.

2. Material & methodology

2.1. Polymer synthesis

Chemically imidizing a poly precursor yielded a polyimide based on HAB-6FDA polyimide [22]. The HAB powder is vacuum dried at 50°C overnight in the absence of light. The 6FDA powder is vacuumed for 30 minutes at room temperature before being subjected to arid air at distinctive weight. The 6FDA is then heat up for 6 hours at 200°C in 10 mmHg vacuum, then overnight at 120°C below complete vacuum. A normal synthesis involved adding 20 mmol of HAB to 44 ml of extracted NMP & stirring by a mechanical stirrer up to the diamine is entirely dispersed. After that, 20 mmol of 6FDA is increased, and the blend is cooled to 5°C and agitated for around 12 hours to create the polymer. To convert polymer to thermally rearranged polyimides, the chemical imidization is a typical approach [23]. Chemical imidization is carried out to make the final polyimide product, the viscous solution from the poly fusion is triggered in methanol and dried up in a vacuum oven at 100°C for 1 day [13].

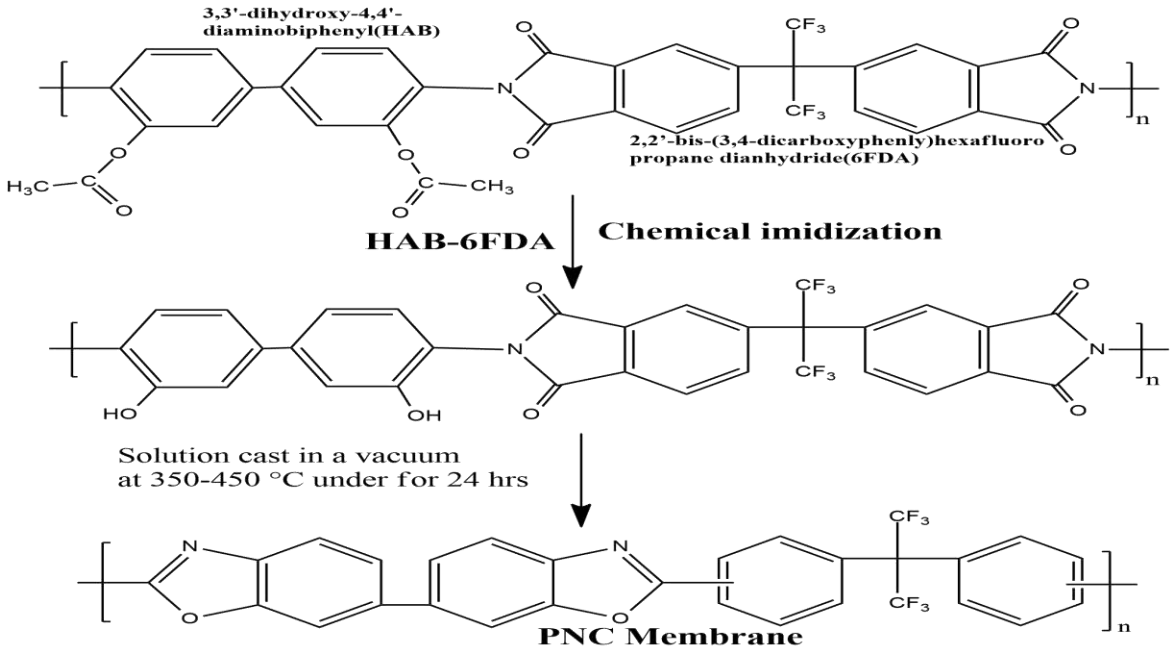

Figure 2: HAB-6FDA polyimide with ortho-functionality chemical structure after thermal rearrangement (TR) process [3].

2.2. Film casting

DMAc solutions with nearly 3% solids are used to cast polymer films by thicknesses ranging from 30 to 50 µ and that filtered solutions are cast onto a flat glass plate with a glass ring connected after passing across a 5 µm polytetrafluoroethylene filter. The concentration of the mixture is added to the casting ring are used to control the film thickness. The films are withered at 80°C overnight in ambient air to evaporate the majority of the solvent and then at 200°C overnight in vacuum to eliminate any remaining DMAc. At last, a film was made by using solution casting method.

2.3. Gas permeation measurements

A constant volume/variable pressure method is used to determine the permeability constants of CH_4, H_2, N_2, CO_2, and O_2 [16]. The gases listed above are listed in the order in which they are tested. The film under investigation is placed in a 47 mm HP Filter Bearer. To determine a definite area, membranes are covered by aluminium tape and glued by epoxy. At feed pressures ranging from 3 to 16 atm, pure gas permeability coefficients are measured. All measurements are carried out at 35°C using Airgas UHP grade fumes [25].

2.4. Thermal rearrangement

First, for thermal rearrangement process the sample at an atmospheric temperature then temperature increased by a rate of 10 °C/ min in a cylindrical heater. Afterward, the samples temperature was reached at 300 °C/ min and steady at that temperature for around 90 min; a short time later, the temperature achieved the ideal thermal rearranged temperature. The membrane film samples were thermally rearranged at atmospheric pressure with an exposed area of approximately 15 cm^2. The membrane films were mounted between two stainless steel plates separated by toric joint and permit the samples to contact but not bend from the center

and boundary sides during the thermal rearrangement process. In this experiment, all the samples prepared by thermal rearrangements were initially at the atmospheric condition and then heated at a 250 °C for 1 hr [2]. The thermal treatment for models used in gas permeability and concentration experiments are developed to replicate the thermal rearrangement to samples, TR tests are heated from ambient conditions to 300°C at a rate of 5°C/min, then kept at 300°C for 1 hour. By this rearrangement technique it's ensures that complete iridization of the sample [26]. The temperature is then risen at a level of 50 °C/min to the required TR heat.

2.5. Permeability, solubility and diffusivity

Permeability in heavy polymer films be able to be explained with the solution-diffusion mechanism [27].

$$P = D \times S \tag{3}$$

Here, D = Diffusion coefficient, P = Gas permeability, S = Solubility coefficient.

The permeability of TR polymers and HAB-6FDA polyimide is tested, and diffusivity values are computed using Eq. 3 using solubility coefficients [27]. The main contributor to the stated rise in gas permeability is the increase in diffusivity with conversion. Conversion raises solubility as well, but not to the same degree as diffusion constants. As, conversion goes from 0 to 76 percent, diffusivity rises with around an order of magnitude for each gas, whereas solubility normally rises by about a binary element.

3. Result and Discussion

3.1 Gas Permeability

Figure 3 shows a constant volume/variable pressure system that describe penetrate flux with using a pressure gauge to observe the pressure rise of accumulated permeate gas in a sealed amount. The entire apparatus is subjected to vacuum and any volatile contaminant in the system can be removed using this procedure. This procedure was used regularly for accessible PC, metal-covered PC, and silica nanocomposite PC films with 10 wt% or 15 wt% filler content. According to Fick's law of diffusion, the data obtained by this method recorded as a function of change of pressure related to time from the downstream side of the gas permeability cell. As outlined in Figure 3, the vacuum determines the slight variation because of gas atoms transportation. Upstream and downstream level are drained with a rotating pump to degas the film. The taps that connected the permeation cell to the vacuum pump are then shut. As a result, pressure will build toward the downstream volume, allowing the system's leak rate to be measured. The leak rate is kept being roughly ten times lower than the steady gas flow. After that, the upstream gas is fed into the cell on the challenging surface of the layer of membrane, plus the pressure increase on the downstream side are measured by using digital pirani gauge as a purpose of time [27].

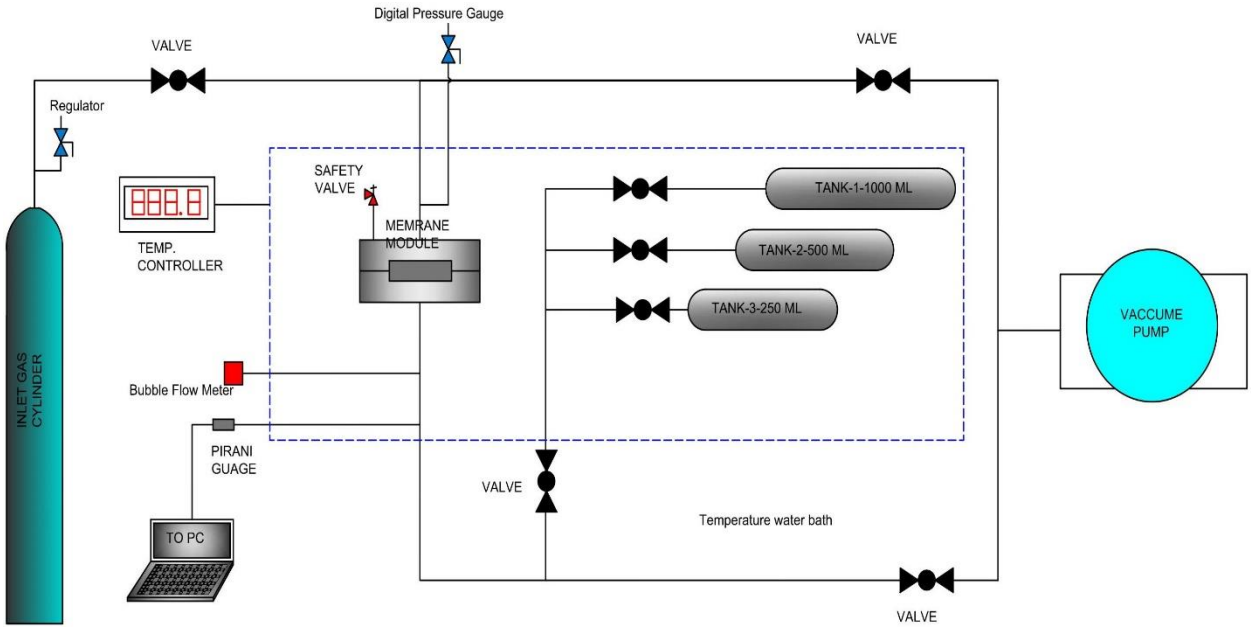

Figure 3 Constant volume/variable pressure system setup.

A constant volume/variable pressure technique are used to determine permeability of different gases like H_2, CH_4, O_2, N_2, gases. The tests are performed at a constant upstream pressure of 30 psi and a continuous heat of 35 °C. This method detects penetrate flux by using a pressure transducer (pirani gauge) to monitor the pressure rise of collected permeate gas in a closed volume. Before talking about the individual measurements, the metal coated and thermally rearranged membranes are arranged in such a way that the coated side is upstream, which is cleaned by penetration gas, & the downstream side of the permeation cell is displaced by the benefit of a rotary pump. The permeability is calculated using the formula below eq.(4):

$$P = \frac{Vd}{pART}(m1) - (m2) \qquad (4)$$

P = Pure gas permeability, m1 = Steady state slope of downstream pressure v/s time calculated in cm-Hg/s, d = Thickness of the membrane, p = Upstream absolute pressure in psig, V = Total volume of downstream side, m2 = Leak rate computed in cm-Hg/s and it was maintained at 10^{-7} cm-Hg/s during the experiment [26]. Permeability was calculated in barrers, where 1 barrer = 10^{-10} [cm^3 (STP) cm/ (cm^2 s cm-Hg)].

In the case of measurement of gas permeability, the gas was applied from the upstream side with a pressure rate of 30 psi toward membranes, which mounted in the permeability cell at 37 ºC temperature. Here, for TR PNC membrane, upstream pressure is around 207 to 275 kPa, and for PNC membranes is approximately 900 to 960 kPa. Using this systems constant volume/variable pressure, we could calculate the gas permeability for different gases like H_2, CH_4, CO_2, N_2, and O_2 [16]. In this system, the capacitance manometer measured downstream pressure (MKS, USA), and upstream pressure measured by a digital pressure gauge in psi (Honeywell, Ohio, USA). The membrane film is mounted in a filter holder with a diameter of 47 mm. This membrane was mounted in a fixed area of permeability cell and partially covered by aluminum foil with a vacuum pump; the downstream pressure was maintained under 2.66 kPa, and output data collected by capacitance manometer with recorded software.

Pure HAB-6FDA polyimides membranes have a higher transfer rate than composite and TR PNC films. The flow rate is comparably affected by other factors i.e., the exposed area, working temperature, membrane thickness. As a result, these variables have an impact on the gas permeation rate. The TR membrane with higher temperature and higher composite rate of nanofiller had the slowest downstream flow rate. When compared to pure polyimide, the H_2 transfer rate of the TR proceed PNC membranes is lower. Expected to difference in the sorption performance of various composition of nanofiller, the flow rate may alter. Gas molecules first interact through a thin layer of nanofiller of hybrid membranes, resulting in a physiochemical reaction. H_2 adsorbed on the composition of nanofiller, fragmented into atomic structure, then dispersed via the metal layer in this process. This rate-deciding step for H_2 diffusion via the nanofiller layer encourages sorption on the membrane's upstream surface. The flow rate also depends on the other parameters such as exposed area, working temperature, thickness of the membrane etc. Hence, these parameters affect the gas transport rate. As a result, the membrane with nanofiller and TR proceed can easily serve as a solution diffusion mechanism's gateway. Furthermore, composite nanofiller increases resistance, which decreases as temperature rises, while the number of unoccupied sites grows as the gas particle enters the material, promoting the diffusion rate in valuable layer permeability [23-26]. As a result, TR proceed composite nanofiller polyimide has a higher flow rate than Pure HAB-6FDA polyimide. The diffusion rate of TR PNC membranes at 35^0C & numerous upstream pressures rate at 30 psi with various gases is shown in Figure. 4. As we observed the downstream pressure has increased as we increased the TR rate of PNC membrane with respect of H_2, CO_2, CH_4, O_2, N_2, gases. The transport rate of different gases through TR 300 °C PNC membrane is shown in Fig. 4.

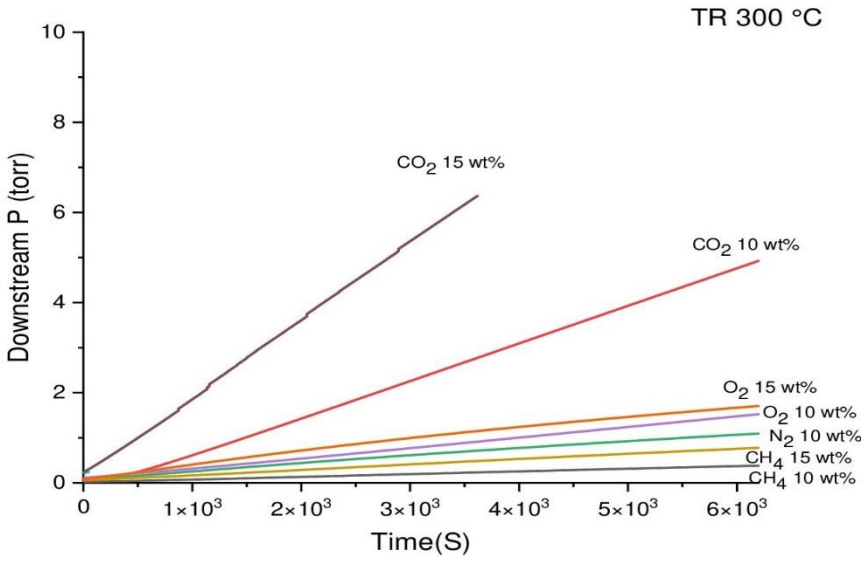

Figure 4 Downstream pressure v/s time for TR 300°C membrane at 30 psi upstream pressure with different gases

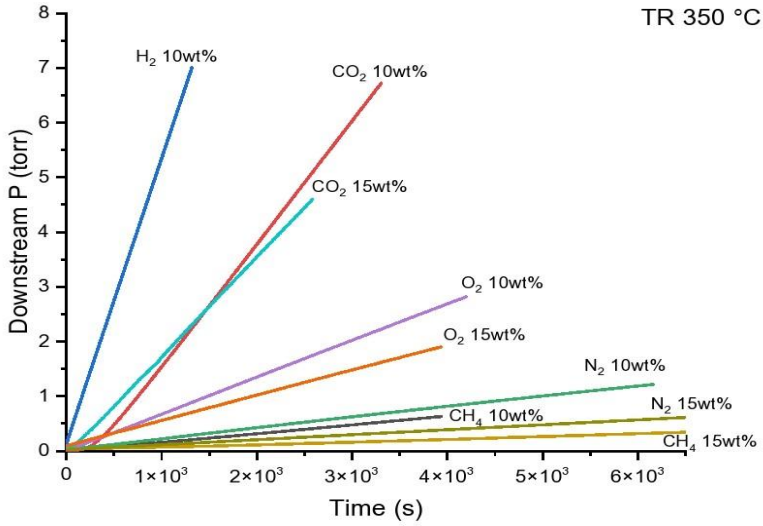

Figure 5 Downstream pressure verses time for TR 350 °C membrane at 30 psi upstream pressure

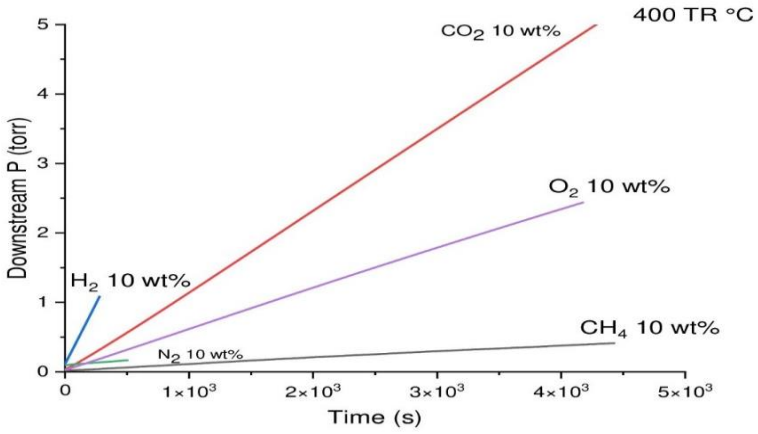

Figure 6 Downstream pressure v/s time for TR 400 °C layer at 30 psi upstream pressure

3.2 Selectivity

Table 1 compare the selectivity of several gas pairings to the allusion values given by Slander et al. Slander's stated work did not include selectivity for H_2/CH_4 and H_2/CO_2, but it is estimated using the consistent permeability values [16].

Table 1: Selectivity contrast of Pure HAB-6FDA (S1), S2+TR 350 °C layers and S1+ 15 wt % silica (S2)

Sample	**H_2/N_2**	**H_2/CO_2**	**H_2/CH_4**
S1+15 wt% silica (S2)	29.01	3.24	54.66
HAB-6FDA (S1)	43.09	1.88	38.30
S1 + TR 350 C	22.62	2.67	49.26

S2 +TR 350 C	34.05	1.81	53.48

The same logarithmic level is used for setting up the trade-off connection among selectivity gas pairs v/s permeability. Equally the upper required limits are calculated [6, 7]. When assessing the selectivity presented in the list for the H_2/CO_2 gas set obtained from the related data to the plain polymer membrane, there is a reduction in magnitude for PNC HAB-6FDA coating. The thermally rearranged HAB-6FDA membrane, on the other hand, has a value that is virtually identical. The PNC TR outcomes in a decline in the partition aspect. Figure 7 described the trade-off between H_2/CO_2 selectivity & H_2 Permeability.

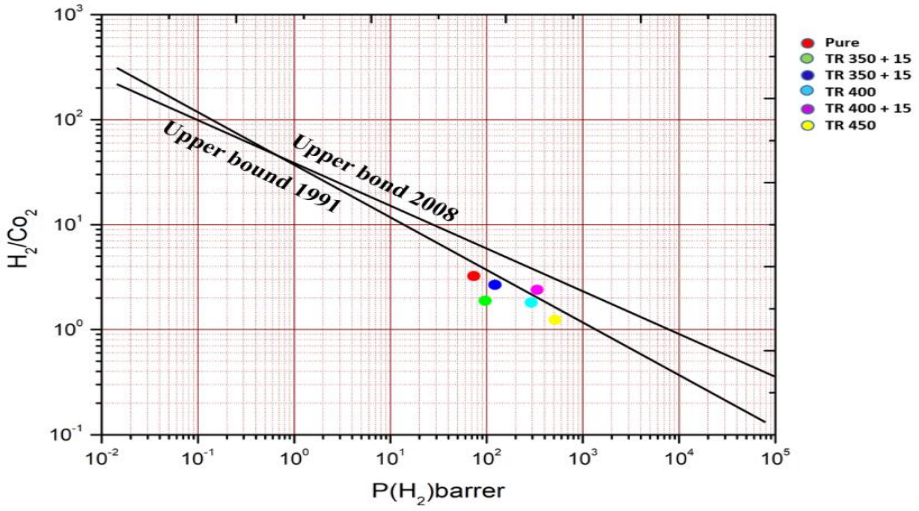

Figure 7 Robeson upper bound correlation for H_2/CO_2 separation.

When contrasted to the other experiments, the selectivity of the PNC membrane decreases. For TR PNC membrane, however, selectivity decreases. The selectivity for this gas set improved by increasing the temperature since insignificant gas molecules are simply disrupted for infiltration when passing through the small holes. The stimulated gas outcomes in improved across the fissures used in the polymer pattern expected to thermal change as the temperature rises [21]. When the temperature rises, sorption capacities decrease due to diminished surface energy, & the activated gas motion outcomes in increased through the holes acquired in the polymer pattern expected to thermal process. As a result, such a membrane might be used to separate H_2 from CO_2. Selectivity is constrained for mutually samples when they are exposed to, H_2/ N_2. When compared to pure polymer, TR PNC's selectivity crosses, as illustrated in Figure. 8. This finding could be used to recover hydrogen from ammonia purge gas, substantial-scale commercial membrane-based gas severance function for periods.

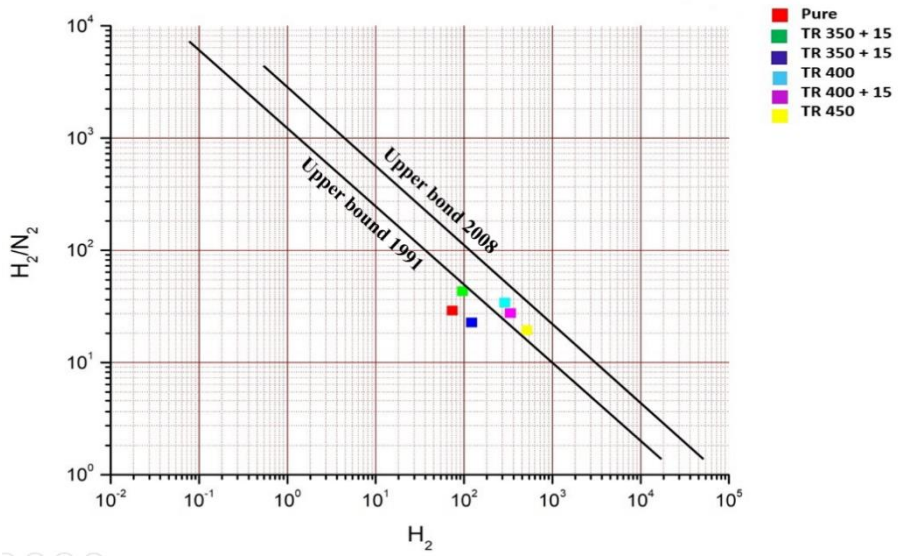

Figure 8: Robeson upper bound correlation for H_2/N_2 separation

The partition of H_2 as of CH_4 is controlled by TR PNC & PNC film in larger amount but it has extra ordinary effect for TR PNC as detected from Figure 9.

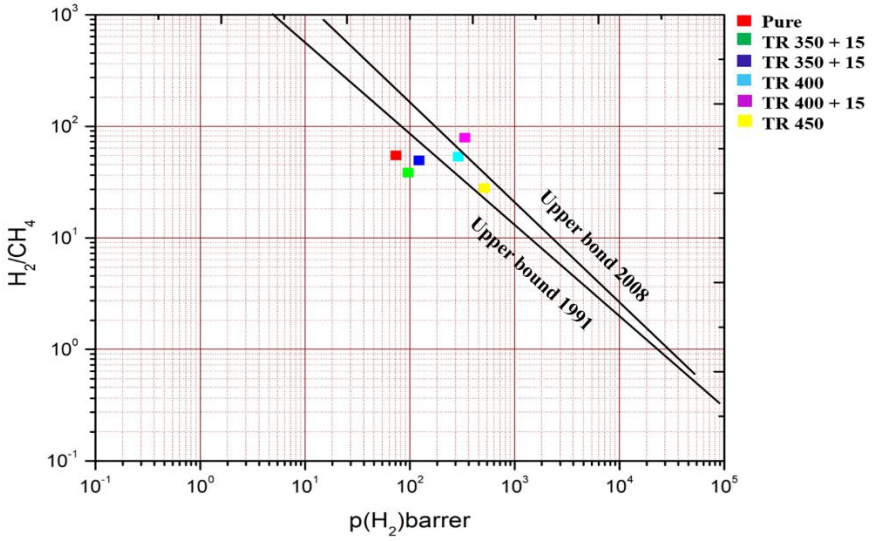

Figure 9: Robeson upper bound correlation for H_2/CH_4 separation

Here, the large amount of separation of H_2 from CH_4 is dominating for PNC membrane and TR PNC membrane with that there is extra ordinary outcome observed from TR PNC which is shown in Fig. 9. Moreover, TR PNC membranes can gives results more purity than PNC membranes. The selectivity of thermally moved nanofiller dispersed upper bound, which is particularly promising for H_2 separation from methane gas functions. Still after distillation, H_2 includes a small quantity of residual CH_4 since it is formed by steam developing hydrocarbons [21]. The TR PNC membrane is capable of separating high pure hydrogen. As a result, the newly designed TR PNC is ideal for separating H_2 from syngas [22]. The H_2 separation method used in factories and petrochemical plants. Gas separation layers, in particular those that separate hydrogen gas, are also used in refineries for oxo-chemical and gas purification fusion [23]. Palladium is normally used to produce elevated purity H_2 gas but expected to several faults in the composition that arise through managing, it is debased by other materials.

3.3 Ultraviolet–visible Spectroscopy

The structure of the thermally rearranged polyimide is validated with UV Spectroscopy, as shown in Figure 10. This experiment were performed by using Thermo Scientific UV Spectroscopy Model Evolution 600 UV-VIS and data analysis by VisionPro software. In this graph it's clearly observed that as we increased the rate of temperature and rate of nanofiller of polyimide membranes there is decrement in rate of transmission of ultraviolet light. Across the TR process, the strength of imide peaks falls [27]. The acetate functionality is dropped in the resulting film, and a hydroxyl group forms in its place. As a result, the emergence of the hydroxyl peak converts the acetate functionality to hydroxy functionality. Also, at around 600 nm there is a drastically change in transmission rate, from that wavelength the rate of transmission is increasing rapidly because of thermal rearrangement process. The result of Uv spectroscopy also reveals chemical interaction between silica nanoparticles and the polymer matrix, with a rise in intensity indicating the presence of silica in the polymer pattern and effect of thermal rearrangement process.

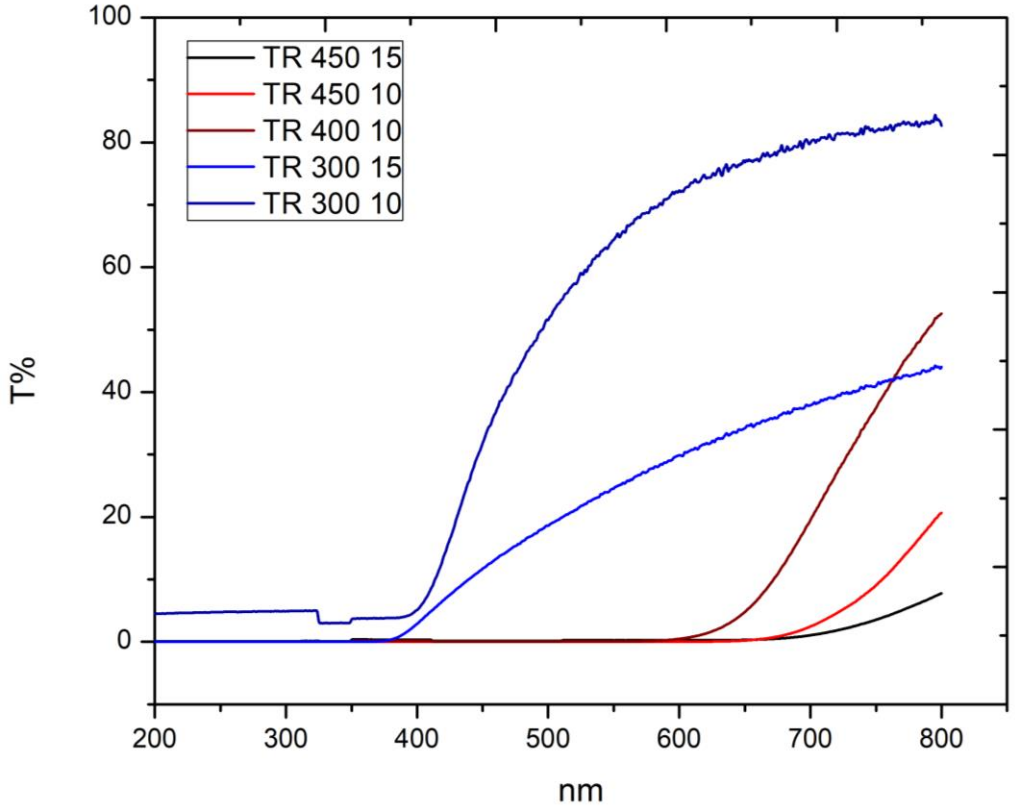

Figure 10: Uv Spectroscopy result of Different Polyimides.

3.4 X-ray diffraction (XRD)

XRD is a method used in materials to define the crystallographic formation of a substance. The crystalline phases of the obtained samples were identified by X-ray diffraction (XRD) by using SmartLab SE powder X-ray diffractometer using a CuKα radiation. XRD functions with exposing a substance plus incident X-rays and determining the scattering plus intensities angles of the X-rays that give the material [17] (Figure 11). XRD is utilized for numerous purposes. For describing crystalline materials, XRD is a potent nondestructive method. Structures, phases, favored crystal alignments, and other mechanical data i.e., average

grain size, strain, crystallinity, and crystal defects are all contained. In this graph it's clearly show this polyimides have crystalline structure.

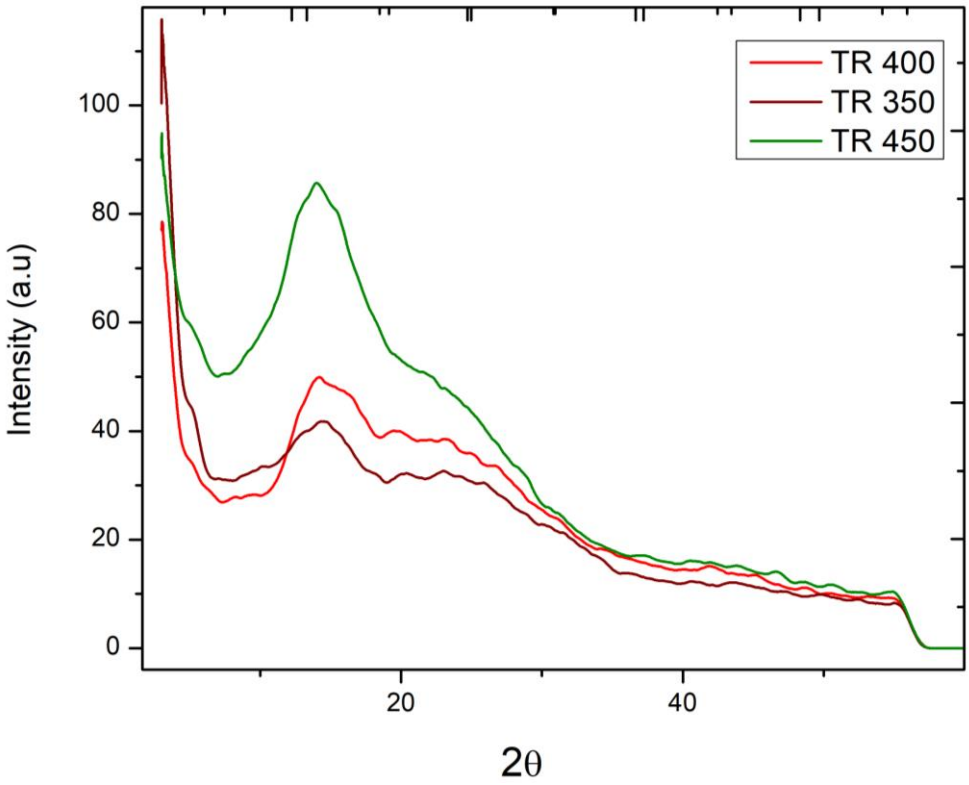

Figure 11: XRD patterns of HAB-6FDA polyimide film showing a relatively higher intensity for the thinner films indicative of more crystalline nature. Same material amount for each film was used for the XRD measurement.

Figure 11 shows the XRD patter of nanocomposite thermally rearranged (TR) polymers with 15 wt % silica, it is clear from the figure that peak position remains almost same up to 450 °C. Therefore, the structural behavior is similar, however the Full width Half Maxima (FWHM) reduces with TR temperature. It was found 24.83 in case of 350 °C, 23.13 for 400 °C and 19.14 for 450 °C that indicates the degree of amorphization. This degree of amorphization is somehow related with the available free volume in the polymer matrix. As a result of this change, nanocomposite membranes exhibit the change in their gas permeabilities.

Conclusion

The emergence of PBO peaks & the elimination of imide peaks owing to TR exchange can be seen in the Uv spectroscopy study. The permeability of glassy polymers diminishes as the kinetic diameter of gases rises, which is a common tendency. The permeability factor of the polyimide remains changed to some extent through the accumulation of silica nanoparticles, though the more substantial for all gases after thermal shift. The composition of silica nanofiller and heat change of the HAB-6FDA coating resulted in amazing performance. In comparison to N_2 and CH_4, the TR adapted nanocomposite has a greater influence on permeability for softer gases as CO_2, & O_2. It lies directly across the upper bound boundary line for the H_2/CH_4 gas pair, which puts the structure in the novel type for gas separation layers. SiO_2 nanoparticles play a critical function in improving H_2 molecule transport modes in this nanocomposite form polyimides. Furthermore, as the amount of silica increases, so does the amount of free space, which improves permeability. Thermal rearrangement process give a better pathway for

penetrants to become soluble in membrane material, resulting in an increase in permeability. Hybridization, it is used to remove H_2 from a gas combination, also maintains the H_2/CO_2 selectivity factor. We get some material who's cross the Robeson's 1991 or 2008 upper limit. XRD pattern reveals that the Full width Half Maxima (FWHM) reduces with TR temperature and it is the consequence of change in gas permeability of these membranes.

Acknowledgement

Authors are thankful to DST-FIST (SR/FST/PSII/2017/20 (C)) of the Applied Physics and DST-Purse scheme of faculty for financial assistance. program of Applied Physics and the author H.D. Patel is thankful to University Grants Commission, New Delhi, for providing fellowship under NET-JRF Scheme (1217/(CSIR-UGC NET DEC. 2018)).

References

[1] Mitchell, Michael J., et al. "Engineering precision nanoparticles for drug delivery." Nature Reviews Drug Discovery 20.2 (2021): 101-124.

[2] Liao, Guan-Ming, et al. "Optimal loading of quaternized chitosan nanofillers in functionalized polyvinyl alcohol polymer membrane for effective hydroxide ion conduction and suppressed alcohol transport." *Polymer* 138 (2018): 65-74.

[3] Bundschuh, Mirco, et al. "Nanoparticles in the environment: where do we come from, where do we go to?." Environmental Sciences Europe 30.1 (2018): 1-17.

[4] Sindhwani, Shrey, et al. "The entry of nanoparticles into solid tumours." Nature materials 19.5 (2020): 566-575.

[5] N. Ben Mansour, W. Djeridi, et. al. "Preparation, Properties and Applications of the Hybrid Organic/ Inorganic Nanocomposite Based on Nanoporous Carbon Matrix" Journal of Inorganic and Organometallic Poly. and Materials. (2021) 31:4360–4371.

[6] Wen, Yue, et al. "Metal–Organic Framework Nanosheets for Thin-Film Composite Membranes with Enhanced Permeability and Selectivity." ACS Applied Nano Materials 3.9 (2020): 9238-9248.

[7] Babak Jaleh, Elham Zare et al. "Preparation and Characterization of Polyvinylpyrrolidone/Polysulfone Ultrafltration Membrane Modifed by Graphene Oxide and Titanium Dioxide for Enhancing Hydrophilicity and Antifouling Properties". Journal of Inorganic and Organometallic Poly. and Materials. (2020) 30:2213–2223.

[8] Huang, Yuan, et al. "Synthesis of chiral conjugated microporous polymer composite membrane and improvements in permeability and selectivity during enantioselective permeation." Separation and Purification Technology 266 (2021): 118529.

[9] Anselmo, Aaron C., and Samir Mitragotri. "Nanoparticles in the clinic." *Bioengineering & translational medicine* 1.1 (2016): 10-29.

[10] Aliofkhazraei, Mahmood, ed. *Handbook of nanoparticles*. Cham, Switzerland: Springer International Publishing, 2016.

[11] Gupta, Akash, et al. "Ultrastable and biofunctionalizable gold nanoparticles." *ACS applied materials & interfaces* 8.22 (2016): 14096-14101.

[12] Stark, Wendelin J., et al. "Industrial applications of nanoparticles." *Chemical Society Reviews* 44.16 (2015): 5793-5805.

[13] Hasan, Saba. "A review on nanoparticles: their synthesis and types." *Res. J. Recent Sci* 2277 (2015): 2502.

[14] Acharya, N. K. "Temperature-dependent gas transport and its correlation with kinetic diameter in polymer nanocomposite membrane." Bulletin of Materials Science 40.3 (2017): 537-543.

[15] Ataeivarjovi, Ebrahim, Zhigang Tang, and Jian Chen. "Study on CO_2 Desorption Behavior of a PDMS–SiO2 Hybrid Membrane Applied in a Novel CO_2 Capture Process." *ACS applied materials & interfaces* 10.34 (2018): 28992-29002.

[16] https://www.lenntech.com/membrane-technology.htm, Membrane Technology, (accessed on 16/June/2021)

[17] Z.P. Smith, D.F. Sanders, C.P. Ribeiro, R. Guo, B.D. Freeman, D.R. Paul, J.E. McGrath, S. Swinnea, Gas sorption and characterization of thermally rearranged polyimides based on 3,3 -dihydroxy-4,4 -diamino-biphenyl (HAB) and 2,2 -bis-(3,4-dicarboxyphenyl) hexafluoropropane dianhydride (6FDA), Journal of Membrane Science, submitted.

[18] Sanders, David F., et al. "Gas permeability, diffusivity, and free volume of thermally rearranged polymers based on 3, 3′-dihydroxy-4, 4′-diamino-biphenyl (HAB) and 2, 2′-bis-(3, 4-dicarboxyphenyl) hexafluoropropane dianhydride (6FDA)." Journal of Membrane Science 409 (2012): 232-241.

[19] Long, Qingwu, et al. "Fabrication of chitosan nanofiltration membranes by the film casting strategy for effective removal of dyes/salts in textile wastewater." *ACS Sustainable Chemistry & Engineering* 8.6 (2020): 2512-2522.

[20] Stennett, Tom E., et al. "Unsymmetrical, cyclic diborenes and thermal rearrangement to a borylborylene." *Angewandte Chemie International Edition* 57.15 (2018): 4098-4102.

[21] Smith ZP, Czenkusch K, Wi S, Gleason KL, Doherty CM, Konstas K, et al. Investigation of the chemical and morphological structure of thermally rearranged polymers. Polymer 2014;55:6649e57.

[22] Guo R, Sanders DF, Smith ZP, Freeman BD, Paul DR, Mcgrath JE. Synthesis and characterization of Thermally Rearranged (TR) polymers : influence of ortho - positioned functional transport properties. J Mater Chem 2013;1:262e72.

[23] Schorer L, Schmitz S, Weber A. Membrane based purification of hydrogen system (MEMPHYS). Int J Hydrogen Energy 2019. https://doi.org/10.1016/j.ijhydene.2019.01.108.

[24] Idris Alamin, Man Zakaria, Maulud Abdulhalim Shah. Polycarbonate/silica nanocomposite membranes: fabrication, characterization, and performance evaluation. J Appl Polym Sci 2017:1-17.

[25] Hyeon Kim Ju, Gyeong Jeon Jei, Ovalle-Robles Raquel, Kang Tae June. Aerogel sheet of carbon nanotubes decorated with palladium nanoparticles for hydrogen gas sensing. Int J Hydrogen Energy 2018;43:645661.

[26] Patel AK, Acharya NK. Study of gas transport phenomenon in layered polymer nanocomposite membranes. In: Nayak K, Mohanty Smita, Unnikrishnan Lakshmi, editors. Trends and applications in advanced polymeric materials. Scrivener Publishing LLC; 2017. p. 191-206.

[27] Patel, A. K., and N. K. Acharya. "Metal coated and nanofiller doped polycarbonate membrane for hydrogen transport." International Journal of Hydrogen Energy 43.47 (2018): 21675-21682.